Journal of Applied Electrochemistry **30**: 217–229, 2000.

An electrochemical study of gold cementation with zinc powder at low cyanide concentration in alkaline solutions

S. VILCHIS-CARBAJAL[1], I. GONZÁLEZ[2] and G.T. LAPIDUS[1]*
[1] *Depto. de Ingeniería de Procesos e Hidraúlica and*
[2] *Depto. de Química, Universidad Autónoma Metropolitana – Iztapalapa, Av. La Purísima y Michoacán s/n, Apdo. Postal 55-534, Mexico, D.F. 09340, Mexico*
*(*author for correspondence, e-mail: gtll@xanum.uam.mx)*

Received 19 January 1999; accepted in revised form 24 August 1999

Key words: cementation, cyanide, Evans' diagrams, gold, zinc powder passivation

Abstract

The half-reactions involved in gold cementation on zinc powder from low concentration alkaline cyanide solutions were studied in a steady state regime, employing electrodes of glassy carbon and graphite paste with zinc powder. The effects of pH, cyanide and initial gold concentrations were investigated using various electrochemical techniques. The results were used to determine the controlling step of the cementation at low cyanide concentration and to interpret the influence of the variables on this process. Mixed potentials and associated currents were determined from the Evans' diagrams constructed using sampled current–potentials curves from chronoamperometric results for half redox reactions. These values do not adequately describe the global cementation reaction because gold reduction in low cyanide concentration solutions is greatly influenced by a strong contribution from adsorptive processes. This behaviour is different from that found by other authors for concentrated gold and cyanide solutions, where the process is controlled by the complex ion diffusion ($Au(CN)_2^-$). The strong component of adsorption found in the present work does not permit the determination, using the Evans' diagrams, of the cementation velocity. Direct monitoring of the mixed potential was proposed, employing an electrode made of zinc powder in carbon paste submerged in a gold cyanide solution. The results of these experiments at low cyanide concentrations show that zinc oxidation is controlled by the formation of different passivating layers, the nature of which depended on the pH of the solution, and that the gold reduction reaction is strongly influenced by adsorption phenomena.

1. Introduction

The extraction of gold from minerals and concentrates with cyanide is an important hydrometallurgical process, which has been studied for more than 100 years [1, 2]. Two of the most important steps in this process are gold leaching in an alkaline cyanide medium, followed by its cementation with zinc powder, carbon adsorption or electrolysis. Generally, in industrial practice, where high concentrations of silver or copper are found, zinc cementation is preferred over the other two processes [3].

One of the most serious problems in the cementation stage is the high cost of reagents. The reduction in concentration of one of them, cyanide, results in an extremely negative consequence, zinc passivation. When this occurs, the controlling step of the process may change and the amount of zinc powder must be increased to raise the gold cementation to an acceptable level [4–6]. There is thus substantial motivation for study of the cementation process under passivating conditions [7].

Most authors have stated that the controlling step in the cementation is $Au(CN)_2^-$ ion transport to the zinc surface [4–9]. On the one hand, all authors employed high cyanide concentrations ($\geqslant 10^{-3}$ M CN^-), which is not common in industrial practice [3]. On the other hand, Eisenmann proposed that the kinetics are dominated first by an adsorption equilibrium, followed by electron transfer [10]. This contradiction in the literature constitutes another reason to study in more detail gold cementation at low cyanide concentrations.

To clarify the passivation problem, an electrochemical study of gold cementation at low cyanide concentrations (10^{-3} and 10^{-4} M) is proposed, which investigates individually each half reaction: gold reduction (cathodic branch) and zinc oxidation (anodic branch) as proposed by Ihsan et al. [4].

$$Au(CN)_2^- + e^- \rightarrow Au^0 + 2\,CN^- \quad (1)$$

$$Zn + 2\,OH^- \rightarrow Zn(OH)_2(s) + 2\,e^- \quad (2)$$

$$Zn(OH)_2 + 4\,CN^- \rightarrow Zn(CN)_4^{2-} + 2\,OH^- \quad (3)$$

Zinc oxidation passes through the intermediate product of $Zn(OH)_2$, whose stability is more important at low cyanide concentrations [4, 5]. The most common procedure is to construct Evans' diagrams, superimposing the anodic and cathodic polarization curves. The crossover point of these curves is thought to determine the mixed potential and current associated with the cementation process. Using these values, in most cases, it is possible to interpret the velocity and controlling step of the cementation [5, 7, 8].

2. Experimental methods

Four electrochemical techniques were used: cyclic voltammetry, electrochemical impedance spectroscopy (EIS), chronoamperometry and direct mixed potential measurement. All experiments were performed in a three electrode cell under a nitrogen atmosphere at a temperature of 30 °C. The electrode arrangement included a saturated sulfate electrode as reference (SSE), a graphite counterelectrode and the working electrode, which was zinc powder in a carbon paste matrix for zinc oxidation or a glassy carbon bar mounted in a Teflon support for the gold reduction studies. Usually, a gold electrode is employed to study gold reduction when Au(I) concentrations are high ($> 10^{-3}$ M), however with the low concentrations used in the present investigation, the capacitative and reductive currents are of the same order of magnitude, camouflaging the nature of the process. Also, since the quantities of gold deposited on the electrode are small, the only way to confirm that a reduction has taken place is studying the oxidation of the recently formed metal over a substrate of a different material, in this case a glassy carbon electrode (GCE). The carbon paste zinc electrode (Zn(CPE)) has the advantage of maintaining the original geometry of the solid species used in the cementation process and for that reason reproducibility is very high [11]. The use of (Zn(CPE)) is even more beneficial than suspended particles because it allows a detailed study of the interface. The zinc powder carbon paste prepared in this study was completely homogeneous. An estimate of the surface area was made by evaluating the geometric area of the electrode (Zn(CPE)) in contact with the electrolyte (3.14×10^{-2} cm^2).

The perturbation signal (potential) and the response (current against potential or current against time) were obtained using a EGG PARC potentiostat (model 273A) linked to a personal computer. Capacity measurements of the glassy carbon cyanide solution interface were performed in the following manner. Initially, impedance diagrams at different imposed potentials were generated in the interval 0.01 Hz to 10 kHz. From these, the frequency was selected where the interfacial capacitative time constant was predominant: (a) 30 Hz for interface (GCE)/solutions containing 0.01 M Na_2SO_4 and 10^{-3} M NaCN at pH 10 and 11 and (b) 10 Hz for the interface (GCE)/solutions containing 0.01 M Na_2SO_4 and 10^{-3} M NaCN at pH 10 and 10^{-6} and 10^{-3} M ($Au(CN)_2^-$). Subsequently, the capacitance–potential diagrams were traced at this frequency. For these studies, the same potentiostat was used coupled with a Solartron (model 1260) frequency response analyser (FRA). Mixed potentials were measured with a millivoltameter (PM2525) controlled by a personal computer. Solutions were prepared with analytical grade chemicals and deionized water. The electrolyte support consisted of 10^{-4} or 10^{-3} M sodium cyanide and 10^{-2} M Na_2SO_4 at pH 10 or 11. The solutions employed for gold reduction additionally contained 10^{-6} to 10^{-3} M $Au(CN)_2^-$. These solution conditions were selected because they represent actual values of industrial operating parameters [3].

3. Results and discussion

3.1. *Gold reduction*

Figures 1 and 2 show the voltamperometric behaviour of a glassy carbon electrode submerged in a solution which contain only cyanide and sodium sulfate. A saturated sulfate reference electrode (SSE, 0.616 V vs NHE) was employed for the entire study which was favoured over chloride since sulfate ion is always present in mineral leach solutions, due to the coexistence of metal sulfides. Figure 1 shows the behaviour of solutions with fixed cyanide concentrations (10^{-4} M, Figure 1(a) and 10^{-3} M, Figure 1(b)) and variable pH (10 and 11). Figure 2 shows the behaviour at fixed pH values (pH 10, Figure 2(a) and pH 11, Figure 2(b)) with variable cyanide concentrations (10^{-4} M and 10^{-3} M). Although these two Figures show the same data, the manner in which the information is combined allows the appreciation of the differences and similarities. The potential scan commences at 0.5 V in the cathodic direction to −2.0 V (direct scan), then, at this potential, the scan is inverted ending in 0.5 V. In the direct scan, a wave is observed at approximately −1.0 V. Because it could not correspond to a faradaic reduction of the electrolytic medium, the wave can only be associated to the adsorption of cyanide. The corresponding current of this wave is more important at pH 10 than at pH 11 for the different concentrations of cyanide (Figure 1). This behaviour is probably due to the competition between the cyanide and hydroxyl ions for adsorption sites on the GCE surface. Alternatively, it may be seen in Figure 2 that, at the same pH, the influence of the cyanide concentration on the adsorption wave is minimal, indicating saturation of the electrochemical monolayer.

To confirm the existence of a capacitative effect at the interface, an impedance study was undertaken at the same conditions. Figure 3 shows the variation of the interfacial capacitance as a function of E (the imposed potential). The interfacial capacitance for pH 11 is lower over the whole potential range. The notable difference

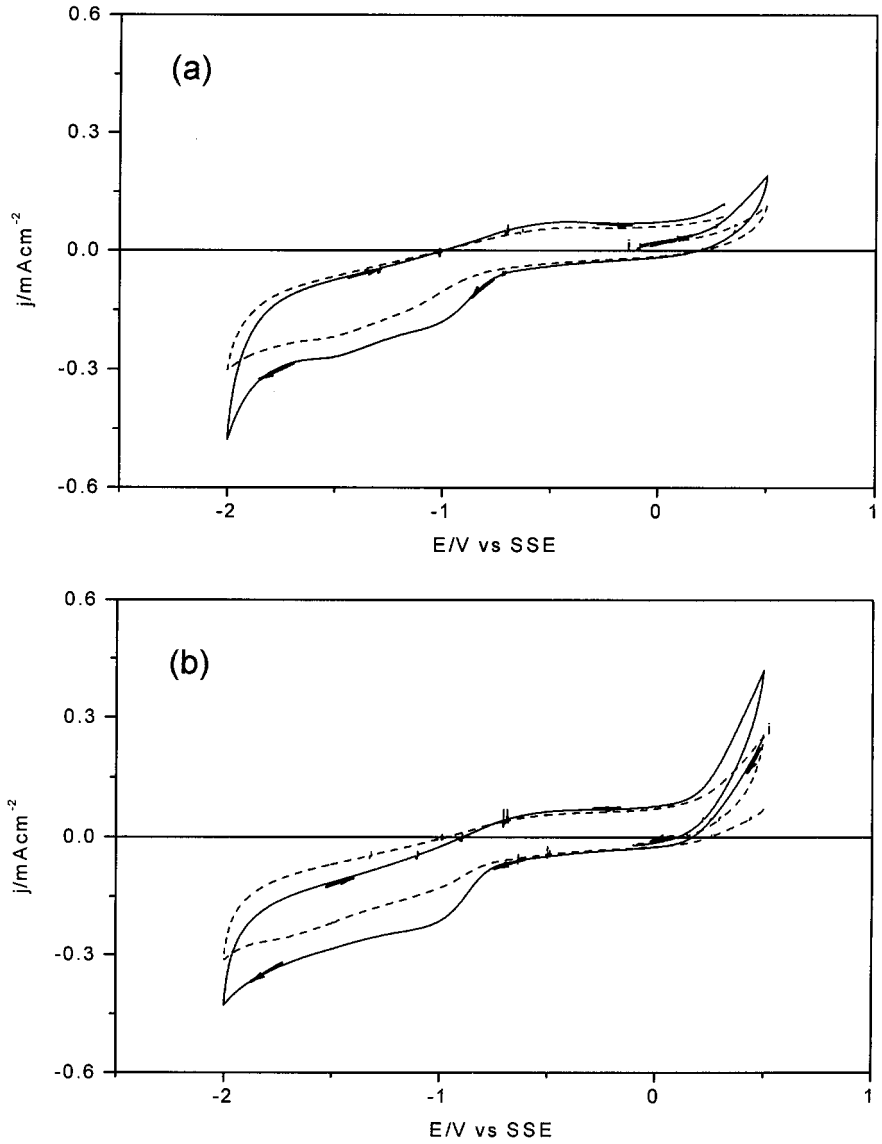

Fig. 1. Typical voltammograms obtained on (GCE) at 50 mV s^{-1} in aqueous solution containing 0.01 M Na_2SO_4, at different pH: (——) 10 and 11 (- - - -). NaCN concentration was modified: (a) 10^{-4} M and (b) 10^{-3} M.

between the capacitance values at both pH indicates a modification of the ions adsorbed at the interface.

In Figure 4, the voltammograms of the supporting electrolyte are compared to those of each solution containing gold (10^{-6}, 10^{-5} and 10^{-3} M) at pH 10 and a constant cyanide concentration (10^{-3} M). The medium adsorption (wave at −1.0 V) is less favourable as the gold concentration increases. Another wave is observed at a potential of −1.8 V for gold concentrations of 10^{-5} and 10^{-6} M, which is independent of the gold concentration (Figure 4 (a) and (b)). This fact and the shape of the peaks suggest adsorption of the gold cyanide complex ($Au(CN)_2^-$). This hypothesis is confirmed by the reduction in interfacial capacitance when $Au(CN)_2^-$ is added to the solution containing 0.01 M Na_2SO_4 and 10^{-3} M NaCN in different concentrations (Figure 5(a) and (b)). When the gold concentration is greater (Figure 4(c)), the controlling step of the electrochemical process changes, modifying the characteristics of this peak. A faradaic reduction of gold exists (peak A), which is evidenced during the reverse scan by the appearance of peak A′ at −0.925 V, representative of gold oxidation (Figure 4(c)). This faradaic reduction provokes a modification of the capacitance of this interface (Figure 5(c)). In this case, the oxidation–reduction process may be represented by Equation 1. The conditional potential associated with this system at the experimental conditions is −1.035 vs SSE [12]. The difference between this value and that of peak A′ is minimal and may be attributed to electrocrystallization processes. Therefore, it may be confirmed that the aforementioned peaks A and A′ correspond to the reduction–oxidation process of $Au(CN)_2^-$.

When gold reduction occurs at high concentrations, water begins to be reduced on the recently formed gold, camouflaging the gold reduction peak (Figure 4(c)). Water reduction on glassy carbon usually takes place at more negative potentials; however, the presence of

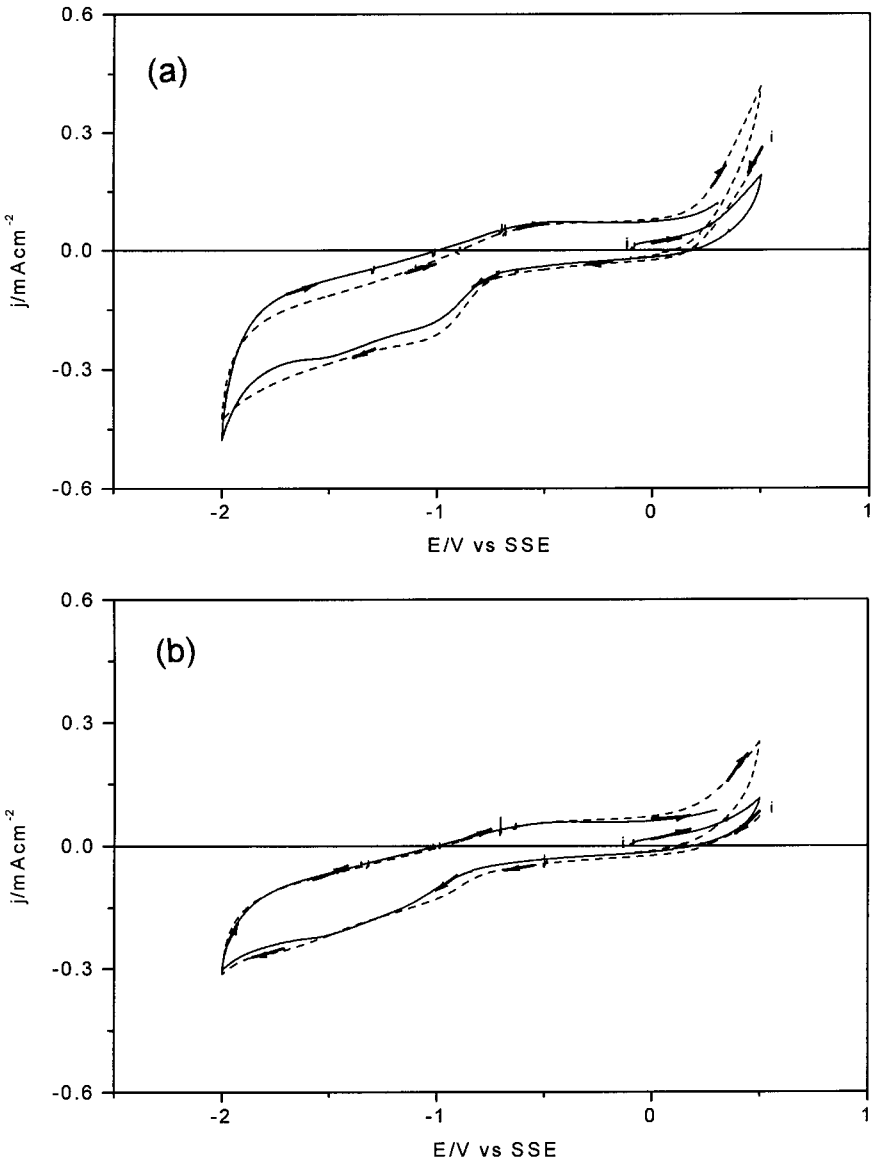

Fig. 2. Typical voltammograms obtained on (GCE) at 50 mV s^{-1} in aqueous solution containing 0.01 M Na_2SO_4, at different NaCN concentration: (——) 10^{-4} M and (- - - -) 10^{-3} M. pH was modified: (a) 10 and (b) 11.

metallic gold shifts the process toward more positive potentials.

To dilucidate the influence of the cyanide concentration, the same study as shown in Figure 4 was carried out at a lower cyanide concentration (10^{-4} M) for the gold cyanide concentrations of 10^{-6} and 10^{-3} M. The voltammograms of Figure 6 show that, even at the high gold concentration (10^{-3} M) (Figure 6(b)), the adsorptive process of the gold cyanide complex is important. The wide peak at −1.8 V still appears at this concentration, indicating that for lower cyanide concentrations, the complex adsorption is greater. However, when the pH is changed from 10 to 11 (Figure 7), the adsorptive effect of the gold complex is suppressed by the competing hydroxyl ions. This contribution may be attributed to the small amount of free cyanide relative to the large quantity of ($Au(CN)_2^-$). In these conditions, a modification of the free cyanide concentration at the interface may be induced when the gold complex is adsorbed or reduced at the surface, which would cause a large variation in the cathodic current when the gold complex concentration or the pH is modified (Figures 6 and 7).

A chronoamperometric study was performed on gold cyanide solutions to verify the presence of large adsorptive effects which mask faradaic processes in the voltamperometric behaviour of the cyanide solutions. When cyclic voltammetry is employed, the energetic properties of the surface are modified with time (dependent upon the potential scan velocity), resulting in a current where the contributions from the energetic changes and the associated reaction velocities are combined. To separate the two types of contributions, chronoamperometry is used. To establish the voltamperometric behaviour of gold reduction without the problems associated with cyclic voltammetry, I/E curves from the chronoamperograms were constructed.

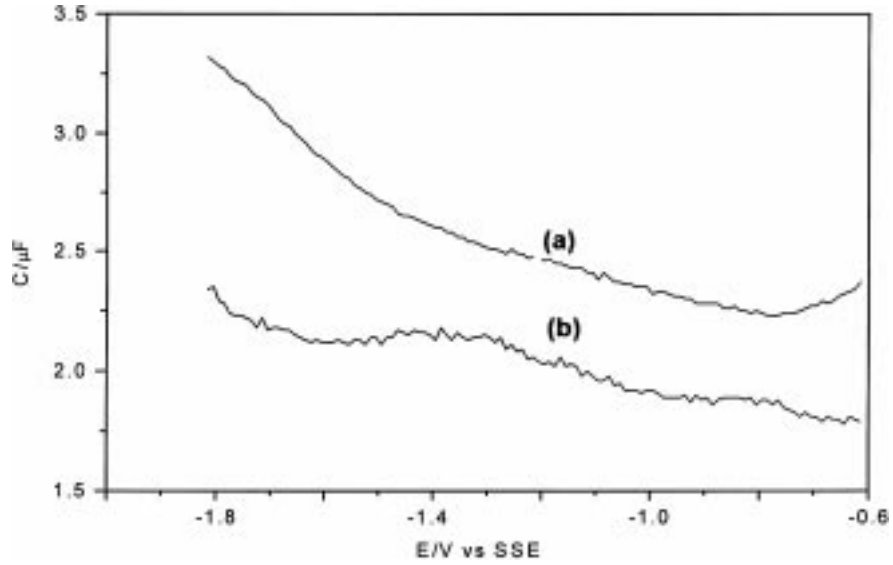

Fig. 3. Variation of the capacitance of the GCE/cyanide solution with the imposed potential. The capacitances were evaluated by (EIS) at 30 Hz at (GCE) immersed in an aqueous solution containing 10^{-3} M NaCN and 0.01 M Na_2SO_4 at different pH: (a) 10 and (b) 11.

Figure 8 shows some of the typical I/E curves constructed for a small sampling time (27 ms) for a low gold concentration (10^{-6} M) and a constant cyanide concentration (10^{-3} M) at pH 10 (Figure 8(a)) and 11 (Figure 8(b)). The selected sampling time for these curves allows observation preferentially of the capacitive contribution to the total current (this capacitive current is directly associated with adsorptive processes). The

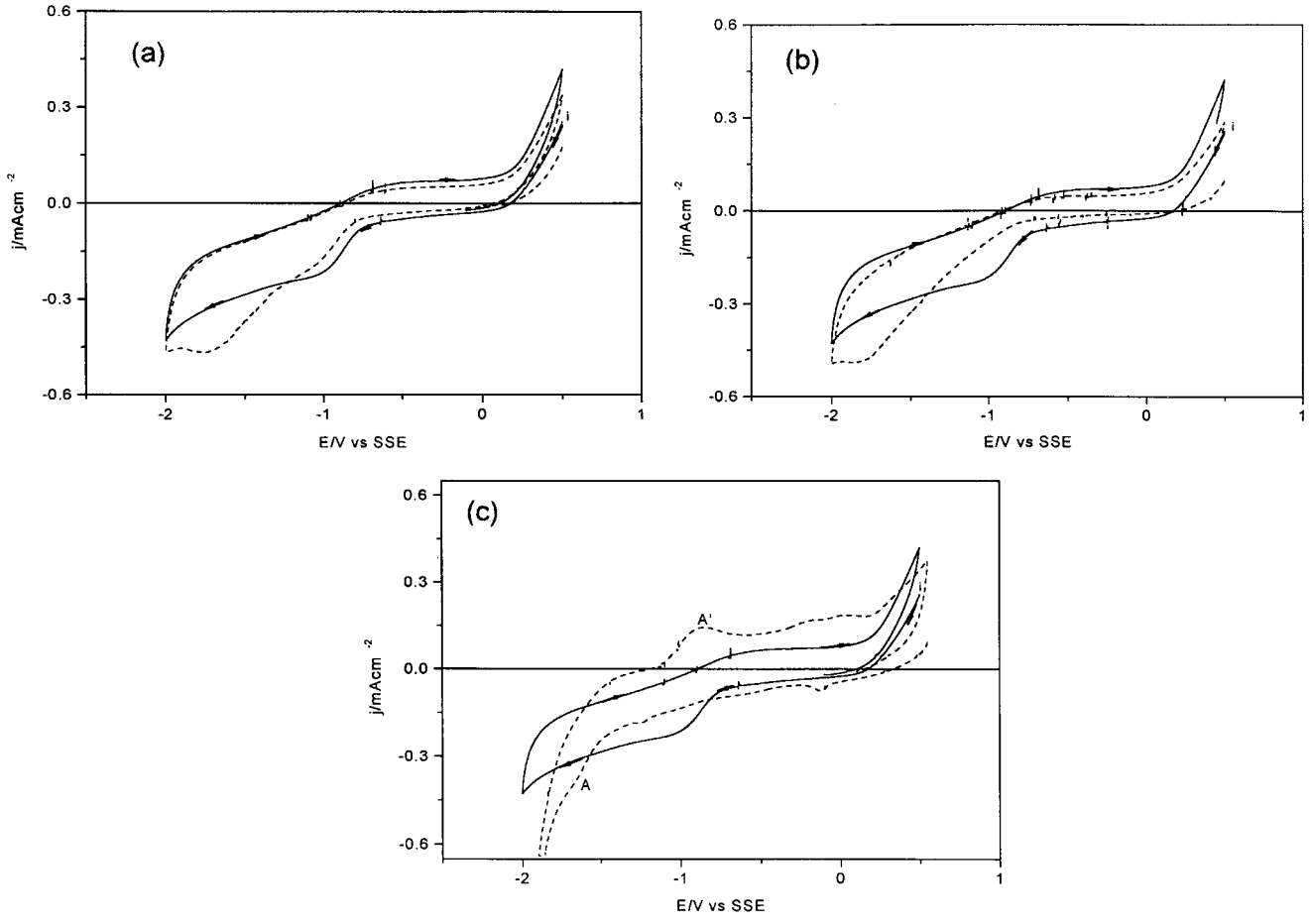

Fig. 4. Comparison between voltammograms obtained in (GCE) (50 mV s^{-1}) electrolytic solution in the absence (——) and in the presence of $(Au(CN)_2^-)$ (- - - -). The electrolytic solution containing 10^{-3} M NaCN and 0.01 M Na_2SO_4 at pH 10. The concentration of $(Au(CN)_2^-)$ was varied: (a) 10^{-6} M, (b) 10^{-5} M and (c) 10^{-3} M.

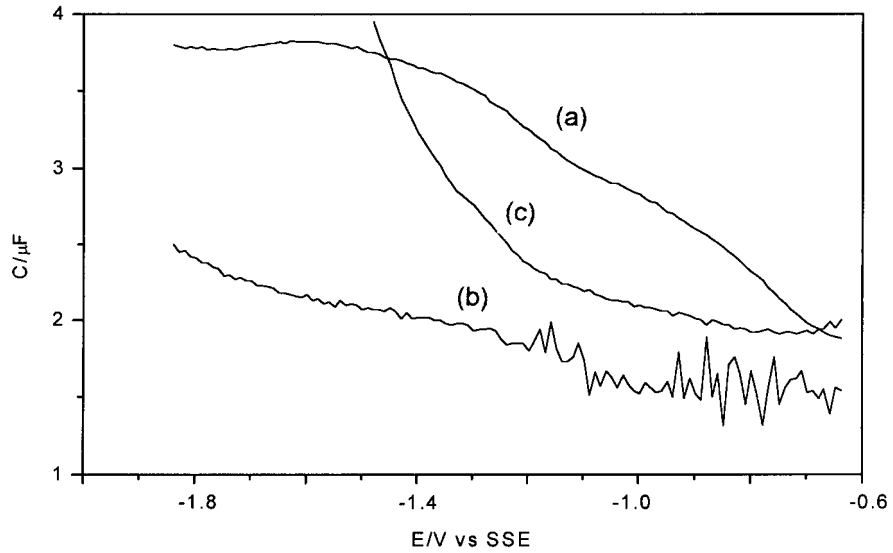

Fig. 5. Variation of the capacitance of the GCE/cyanide solution with an imposed potential. The capacitances were evaluated by (EIS) at 10 Hz at the (GCE) immersed in an aqueous solution containing 10^{-3} M NaCN and 0.01 M Na_2SO_4 at pH 10 and different concentrations of ($Au(CN)_2^-$): (a) 0, (b) 10^{-6} M and (c) 10^{-3} M.

associated current is greater at pH 11 (Figure 8(b)). The same behavior was observed with larger sampling times (up to 5 s), however the response is amplified at this short time. Since the Au(I) concentrations are identical in both solutions, this difference is indicative of a modification in the adsorptive processes. In Figure 9, I/E curves for solutions with different concentrations of gold (Figure 9(b) and (c)) and without gold (Figure 9(a)) are shown at pH 10 and at a constant cyanide concentration (10^{-4} M). If the current were due exclusively to faradaic processes, this would be expected to increase with the gold concentration. However, the associated current actually decreases for the highest gold concentration to a value lower than when there is no gold present (supporting electrolyte). This indicates that the adsorptive effects are more important than the faradaic ones. It may be concluded that the corresponding gold reduction current has an important contribution from adsorption processes that does not allow the exact determination, by these methods, of the faradaic current that is associated with metallic gold formation. This behaviour is due to the low cyanide concentration, which differs from the findings of other authors [5, 7], who worked at high cyanide concentrations.

3.2. *Zinc oxidation*

The behaviour of the (Zn(CPE)) was studied in solutions containing 0.01 M Na_2SO_4 and 10^{-3} M NaCN at pH 10. The presence of sulfates modifies the oxidation–reduction behaviour of zinc relative to that reported in solutions containing only cyanide. However, because of the very small quantity of cyanide employed, the use of a supporting electrolyte was necessary.

In electrochemical studies that involve solid species it is important to start from the open circuit potential (OCP) to obtain reproducible results. The (OCP) was determined by monitoring the working electrode potentials starting from the time when the solution was first introduced until the potential remained stable. The time for the system to reach this potential is called the 'solution conditioning time'. The OCP at pH 10 is −1.25 V, while the (OCP) for the solution at pH 11 is −0.6 V. Additionally, there exists a large difference in conditioning time (5 min at pH 10 and 15 min at pH 11). This indicates that the cyanide solution interacts in a different manner with the zinc surfaces at the two pH values. Other authors [4, 5] have observed that at low cyanide concentrations a zinc hydroxide layer is formed which should be of a different nature at pH 10 than at pH 11.

Figure 10 shows typical voltammograms obtained on a graphite paste electrode containing zinc powder (Zn(CPE)) in aqueous cyanide media at pH 10 and 11. The potential scans commence at the (OCP) and proceed to 0.8 V (direct scan), at which point the potential scan is inverted and brought back to −2.0 V (reverse scan). In the direct scan (anodic), a large oxidation peak is observed (B′ and B1′), which may be associated with the formation of zinc hydroxides that passivate the metal surface [4, 5] due to the low cyanide concentration (Equations 2 and 3). When the potential is inverted, the formation of these hydroxides continues since an oxidation current still exists in the inverse scan. When the potential is more negative (−1.7 V), a small peak appears which corresponds to the reduction of the zinc that had been dissolved in the oxidation process. This last statement is supported by the fact that said peak disappears when the solution is agitated or when the potential scan is initiated in the opposite (cathodic) direction. Finally, the process observed in the limit of the cathodic scan is due to water reduction.

The currents associated with the oxidation–reduction processes of zinc are greater at pH 11. However, to

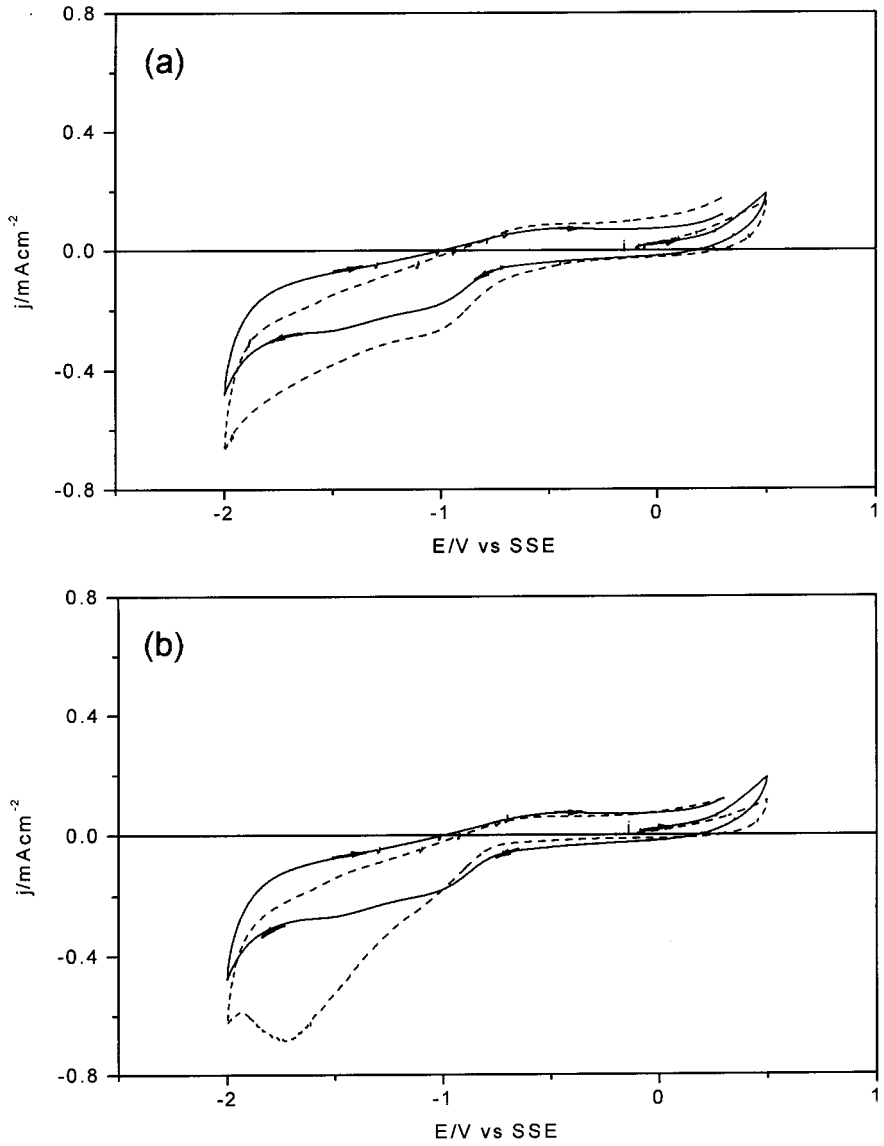

Fig. 6. Comparison between voltammograms obtained in (GCE) (50 mV s^{-1}) electrolytic solution in the absence (——) and in the presence of ($Au(CN)_2^-$) (- - - -). The electrolytic solution containing 10^{-4} M NaCN and 0.01 M Na_2SO_4 at pH 10. The concentration of ($Au(CN)_2^-$) was varied: (a) 10^{-6} M and (b) 10^{-3} M.

obtain a large current for zinc dissolution at this pH, more positive potentials are required than those needed at pH 10 (B′) and (B1′). The differences in the current magnitude and the potential of the oxidation peak (B1′) obtained at pH 11 with respect to peak (B′) at pH 10, leads to the supposition that the surface of zinc hydroxide at the two pH's are different. The large oxidation current in the inverse scan, more pronounced for pH 11 than for pH 10, indicates that the passive layer of zinc hydroxide formed at pH 11 continues to dissolve at more negative potentials, probably due to the higher concentration of hydroxyl ions. This hypothesis is confirmed by peak (C), much larger for pH 11, which represents the reduction of soluble Zn(II), recently oxidized in the direct potential scan. When the scan is inverted at −2.0 V, peak C′ is obtained, but only for pH 11. This peak appears at a less negative potential (−1.05 V) than the other oxidation peaks (B′ and B1′) and is associated with the metallic zinc, recently formed in the reduction process represented by peak C. The half potential $E_{1/2}$ ($E_{pc} + E_{pa}/2$) from peaks C and C′ is −1.47 V vs SSE, comparable to the conditional potential associated with this system ($Zn(OH)_2/Zn$) at these experimental conditions (−1.622 V) [12], confirming the hypothesis that peaks C and C′ correspond to the zinc oxidation–reduction system.

It may be assumed that at this low bulk cyanide concentration and with the large rate of zinc dissolution, the interfacial cyanide may be limited. In this situation, the solubility of the superficial zinc hydroxide is a function of both the cyanide and the hydroxyl ion concentrations, as may be calculated from the complex stability constants and the zinc hydroxide solubility product [13]. Under these conditions, zinc hydroxide would be more soluble at pH 11 than at pH 10.

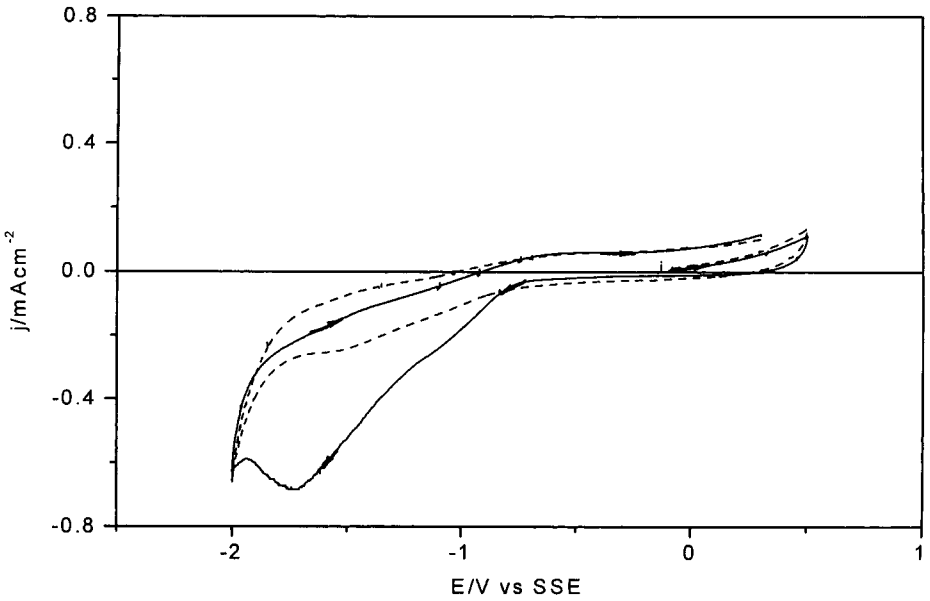

Fig. 7. Typical voltammograms obtained on (GCE) at 50 mV s^{-1} in aqueous solution containing 10^{-3} M $Au(CN)_2^-$, 10^{-4} M NaCN and 0.01 M Na_2SO_4, at different pH: (——) 10 and (- - - -) 11.

The potential and characteristics of peak C′ are totally different from those observed for peaks B′ and B1′. This confirms that the zinc powder employed in the carbon paste initially has a passive layer which requires an overpotential to dissolve it, even at a high pH value. The crossover potential of zinc oxidation and gold reduction occurs near the zinc (OCP). Since the objective of this research is to study the cementation process, the behavior of the passive layer in this zone is required.

In the voltammograms for pH 10 and 11 (Figure 10), no appreciable changes in oxidation current are observed near the (OCP) due to the limitations of this technique. To separate the contributions from the energetic changes and the associated reaction velocities, it is necessary to use the chronoamperometric technique performed in the potential range corresponding to potentials less negative than that of the (OCP) (–0.8 to −1.25 V). In Figure 11, the I/E curves constructed at different sampling times are shown for the oxidation of (Zn(CPE)) in the supporting electrolyte at pH 10 and 11. While the I/E curves obtained with cyclic voltammetry show very little difference between the two pH values near their (OCP)'s, in the I/E curves, a sizeable difference may be observed.

The currents associated with zinc oxidation at pH 11 are more important than those at pH 10. In both cases, oscillations are observed which probably correspond to oxidation–passivation processes. The associated cur-

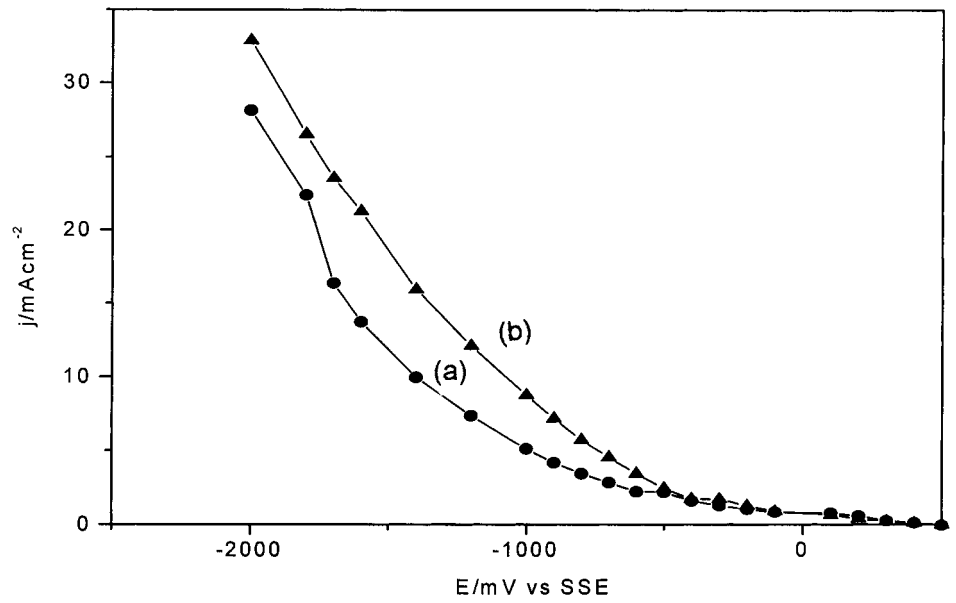

Fig. 8. Sampled current–potential constructed from potentiostatic current transients obtained on (GCE) in aqueous solution containing 10^{-6} M $Au(CN)_2^-$, 10^{-3} M NaCN and 0.01 M Na_2SO_4, at different pH: (a) 10 and (b) 11. Current was sampled at 27 ms.

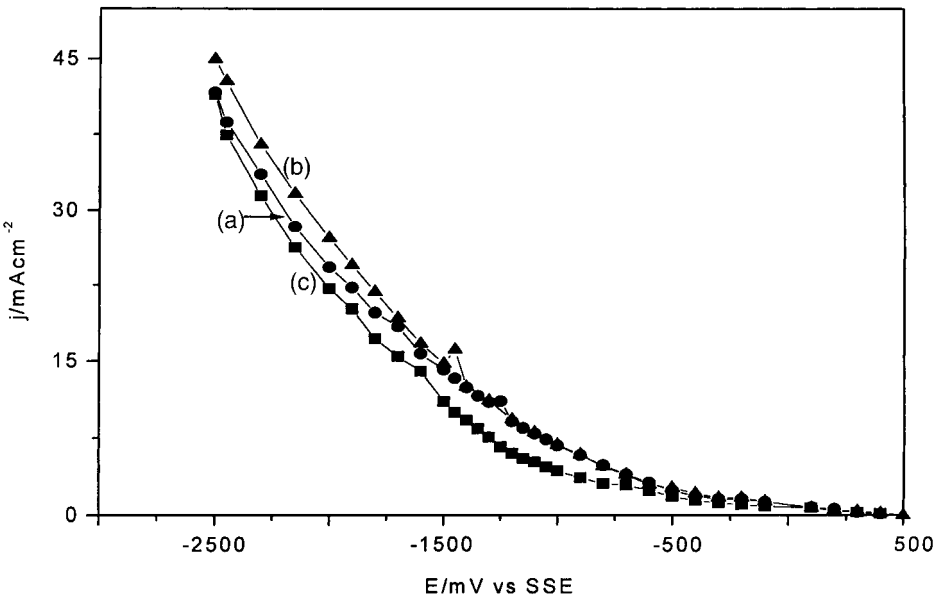

Fig. 9. Sampled current–potential constructed from potentiostatic current transients obtained on (GCE) in aqueous solution contained 10^{-4} M NaCN and 0.01 M Na_2SO_4, at pH 10 at different ($Au(CN)_2^-$): (a) 0, (b) 10^{-6} M and (c) 10^{-3} M. Current was sampled at 27 ms.

rents diminish as the sampling time increases, indicating that the oxidation process is strongly affected by diffusion. These modifications with time are also noted at pH 10, however, they are not perceivable in the Figure due to the large difference in magnitude between the currents at pH 10 and 11. In the I/E curves of Figure 11, the abrupt increments are related to zinc oxidation and the sharp decreases to passivation. At pH 11 the magnitude of the oscillations become more important as the potential is less negative. For less basic pH values the oscillations are minimal, denoting a more constant process. This behaviour indicates that the nature and character of the passivating layers formed at pH's 10 and 11 are quite different, confirming the observations made in the voltammograms (Figure 10). From the previous discussion it is possible to explain why, even at the (OCP), the (Zn(CPE)) potential is variable at more basic values of pH.

3.3. *Evans' diagrams*

The ultimate purpose of studying the anodic behavior of zinc and the cathodic behavior of gold is to generate Evans' diagrams to evaluate the potential and velocity of cementation. For the case analysed here, such diagrams were constructed employing the current–

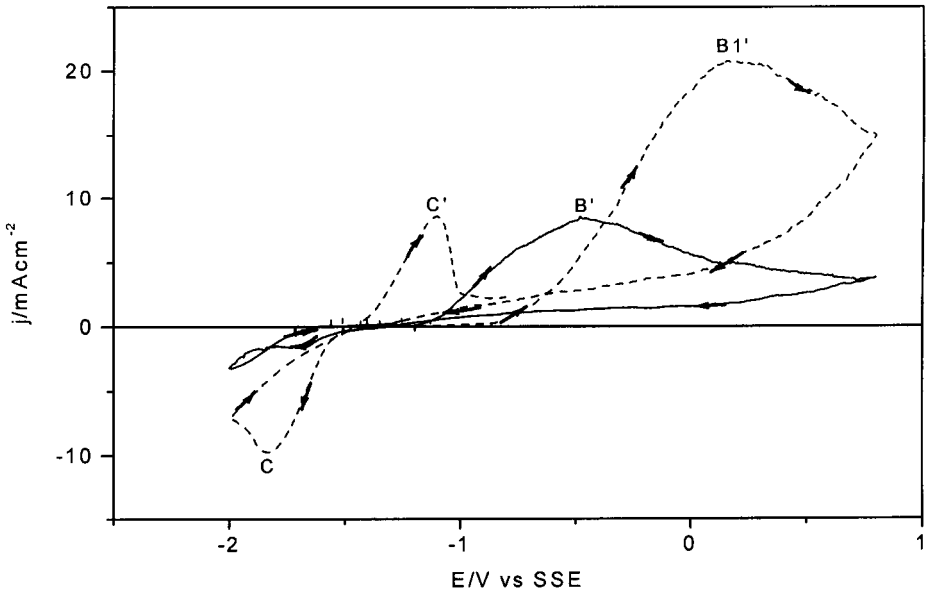

Fig. 10. Typical voltammograms (50 mV s^{-1}) obtained for metallic zinc in CPE (Zn(CPE)) in aqueous solution containing 10^{-3} M NaCN and 0.01 M Na_2SO_4, at different pH: (——) 10 and (- - - -) 11. The scan was initiated from OCP (−1.25 V at pH 10 and −0.6 V at pH 11) to anodic direction.

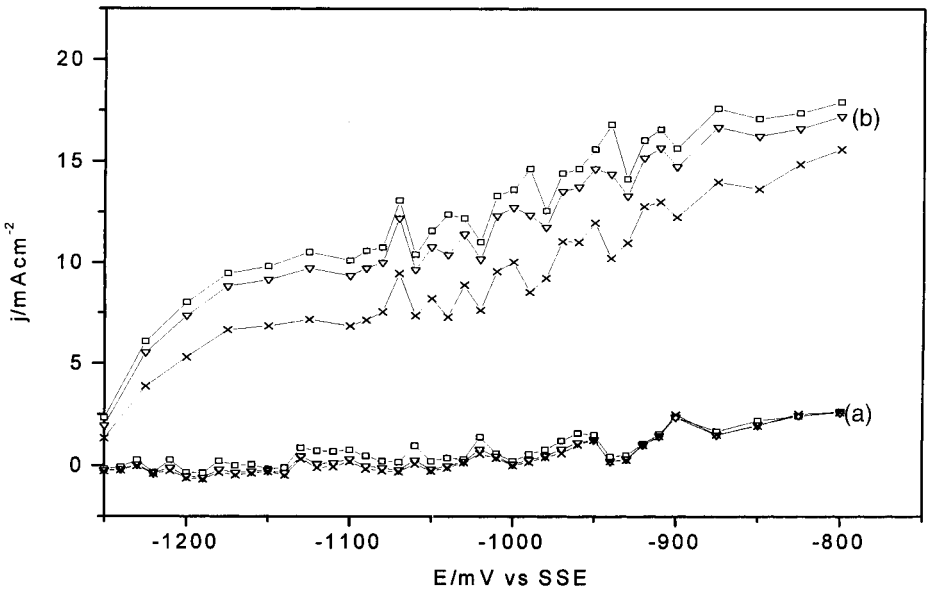

Fig. 11. Sampled current–potential constructed from potentiostatic current transients obtained on metallic zinc in CPE (Zn(CPE)) in aqueous solution containing 10^{-3} M NaCN and 0.01 M Na_2SO_4, at different values of pH: (a) curves at 10 and (b) curves at 11. Current was sampled at different times: (□) 27, (▽) 54 and (×) 74 ms.

potential (I/E) curves obtained from the series of chronoamperograms for each half-reaction. Figure 12 shows a typical diagram generated in this work. The zone where the I/E curves cross defines the controlling step (adsorption, charge transfer or diffusion). The mixed potential is that where the velocities of the anodic and cathodic reactions are equal, which signifies that no net current is present. The anodic or cathodic current in this point would correspond to the cementation velocity.

Table 1 shows the crossover potentials and currents obtained from the corresponding Evans' diagrams at different conditions. At 10^{-3} M cyanide and gold concentrations equal to or larger than 10^{-5} M, three crossover points are found due to the oscillations caused by the zinc oxidation–passivation process. The crossover potentials and currents are essentially the same for the supporting electrolyte and for all the gold concentrations. This suggests that the controlling step of the cementation is zinc oxidation and not gold reduction. However, the crossover potentials at these conditions are near the cyanide adsorption wave (Figure 1). Additionally, it was demonstrated that at pH 11 the cyanide adsorption wave was suppressed and, consequently, the mixed potential was shifted to more negative values

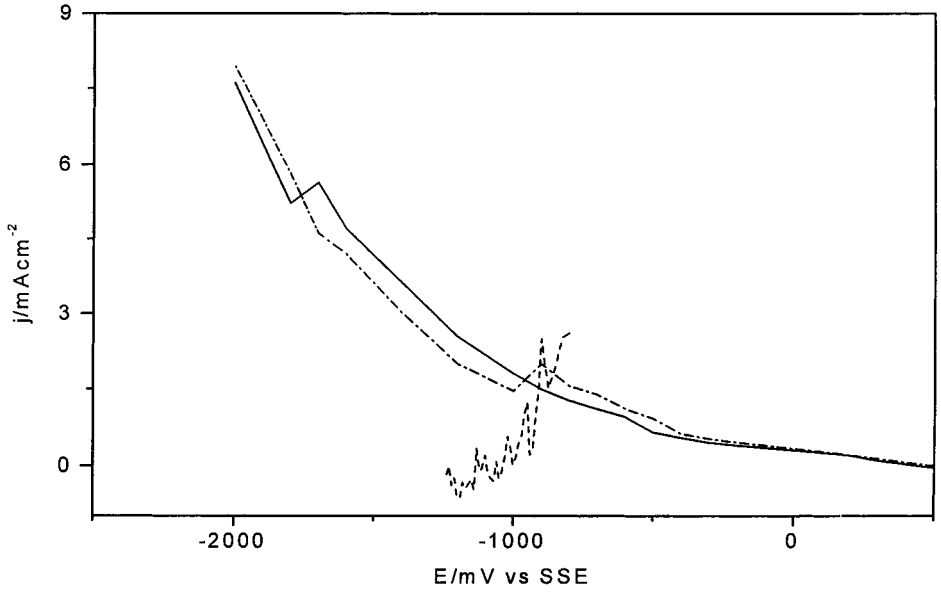

Fig. 12. Evans' diagrams for the redox system ($Zn/Au(CN)_2^-$) for the gold cementation by zinc in an aqueous solution containing 10^{-3} M NaCN and 0.01 M Na_2SO_4 at pH 10. The I/E curves were constructed from the corresponding potentiostatic current transients and the current were sampled at 27 ms. The zinc oxidation (- - - -) was obtained from Zn(CPE) and the gold reduction curves were obtained at different concentrations of ($Au(CN)_2^-$): (——) 10^{-6} M and (– – – -) 10^{-5} M.

Table 1. Crossover potentials and currents obtained from the corresponding Evans' diagrams in solutions containing 0.01 M Na_2SO_4 and 10^{-3} M NaCN at pH 10, the zinc oxidation was obtained from Zn(CPE) and the gold reduction curves were obtained at different ($Au(CN)_2^-$) concentrations*

($Au(CN)_2^-$)/M	E/mV	I/μA
0 (Sup. elect.)	−909	−46
10^{-6}	−909	−45
10^{-5}	−858	−49
	−887	−60
	−906	−63
10^{-4}	−872	−46
	−878	−46
	−908	−47
10^{-3}	−854	−60
	−859	−65
	−905	−67

* The Evans' diagrams were constructed from sampled I/E curves at a sample time of 74 ms.

(Table 2). This confirms that the adsorption camouflages the gold reduction process. For this reason, these potential and currents do not describe the conditions of the cementation process since at the mixed (crossover) potential it is not possible to observe the faradaic contribution of gold. These results differ from those found by other authors who studied this system at higher cyanide concentrations, where gold reduction is limited by diffusion [5, 7].

It may be concluded that in processes where adsorption takes on a predominant role (for example in systems such as $[Au(CN)_2^-]/Au^0$, [Ag + ethylamine]/glassy carbon) [14–16], evaluation of the cementation velocity and the controlling step by means of Evans' diagrams is not reliable. Consequently, the results produced with the techniques employed do not allow the precise determination of the cementation velocity. Because of this, the direct determination of the mixed potentials of the $Au(CN)_2^-/Zn^0$ system was necessary in order to clear up those points where the validity of Evans' diagrams is limited.

3.4 *Mixed potential of* $(Au(CN)_2^-)/Zn^0$ *system*

The mixed potential of the $Au(CN)_2^-/Zn^0$ system should not be confused with the oxidation–reduction potential (ORP) of the solution. The former measures the interfacial potential where the cementation process takes place, while the latter detects the redox properties of the cementation solution (the (ORP) of the solution is determined using a platinum electrode). The mixed potential may be measured with a solid zinc bar, however, its superficial characteristics are completely different from those of zinc powder used in the industrial process. In order to approximate those conditions, a carbon paste electrode with this powder (Zn(CPE)) was used.

Table 2. Crossover potentials and currents obtained from the corresponding Evans' diagrams in solutions containing 0.01 M Na_2SO_4 and 10^{-3} M NaCN at pH 11, the zinc oxidation was obtained from Zn(CPE) and the gold reduction curves were obtained at different ($Au(CN)_2^-$) concentrations*

($Au(CN)_2^-$)/M	E/mV	I/μA
0 (Sup. elect.)	−1232	−101
	−1269	−106
	−1323	−111
10^{-6}	−1232	−104
	−1271	−111
	−1303	−116

* The Evans' diagrams were constructed from sampled I/E curves at a sample time of 74 ms.

The change in potential with respect to time was determined using the (Zn(CPE)) electrode in the presence of different electrolytes with distinct pH values and concentrations of gold and cyanide. In Figure 13, the potential–time (E/t) curves are shown for the $Au(CN)_2^-/Zn^0$ system at different gold concentrations in 0.01 M Na_2SO_4 and 10^{-4} M NaCN at pH 10. In Figure 14, the corresponding curves are plotted for the same conditions as before, but with a higher cyanide concentration (10^{-3} M).

At both cyanide concentrations (Figures 13(b) and 14(b)), oscillations in the value of the mixed potential are observed at pH 11. These oscillations are larger when the cyanide concentration is low (Figure 13(b)). Oscillations in the potential are indicative of an oxidation–passivation process probably due to the flaking of the passive layer. The absence of oscillation in the (E/t) curves at pH 10 (Figures 13(a) and 14(a)) imply that considerable flaking does not exist at this pH, corroborating that the passive layer is more stable. The values of the mixed potential are more negative with respect to those obtained at pH 11 for both cyanide concentrations. This difference between the mixed potentials at the two pH's suggests that a distinct phenomena may be controlling the cementation process at each pH. A pH 11, the controlling step may probably be zinc oxidation–passivation.

The oscillations observed in the intensity–potential curves generated from the chronoamperometric study of (Zn(CPE)) in cyanide solution (Figure 11) (where the oxidation is provoked electrically) are similar to those observed in Figures 13 and 14, where zinc oxidation is chemically induced by the cementation reaction.

For both levels of cyanide, the mixed potential becomes less negative as the gold concentration increases (Figures 13 and 14). These variations indicate that at pH 10 the controlling step is the gold reduction. This reduction is affected by the adsorptive processes of cyanide and of the gold cyanide complex, illustrated by the difference in the E/t behaviour when the cyanide concentration is modified at the same gold concentration and pH.

In this manner it can be shown that while the adsorptive effects do not allow the obtention of information on the gold reductive processes from the Evans' diagrams, the evaluation of the mixed potentials permit the detection of variations in the cementation process when the conditions are modified. Figures 13 and 14 suggest that the cementation process presents optimum

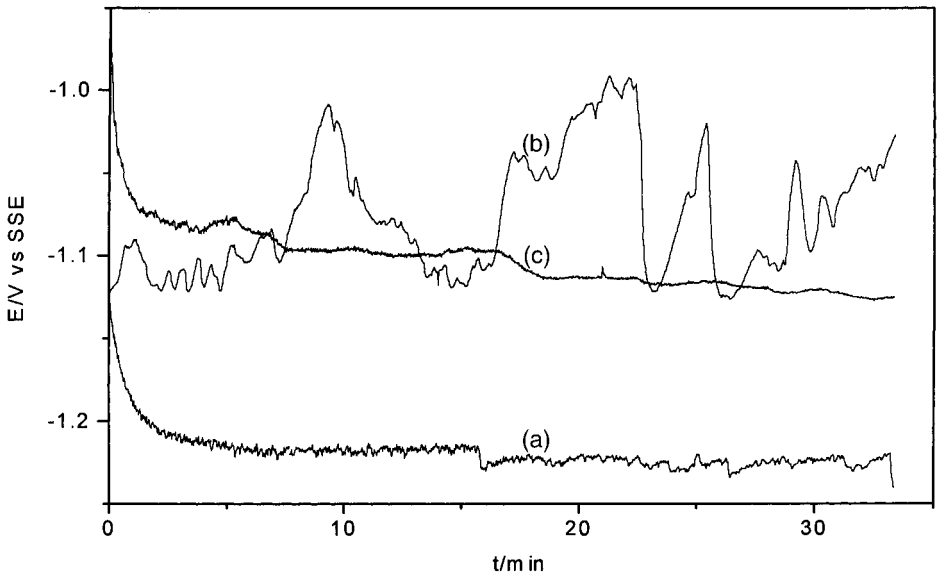

Fig. 13. Variation of the mixed potential of metallic zinc in CPE (Zn(CPE)) with the immersion time in aqueous solution containing 10^{-4} M NaCN and 0.01 M Na_2SO_4 at different concentrations of $(Au(CN)_2^-)$ and pH: (a) 10^{-6} M at pH 10, (b) 10^{-6} M at pH 11 and (c) 10^{-3} M at pH 10.

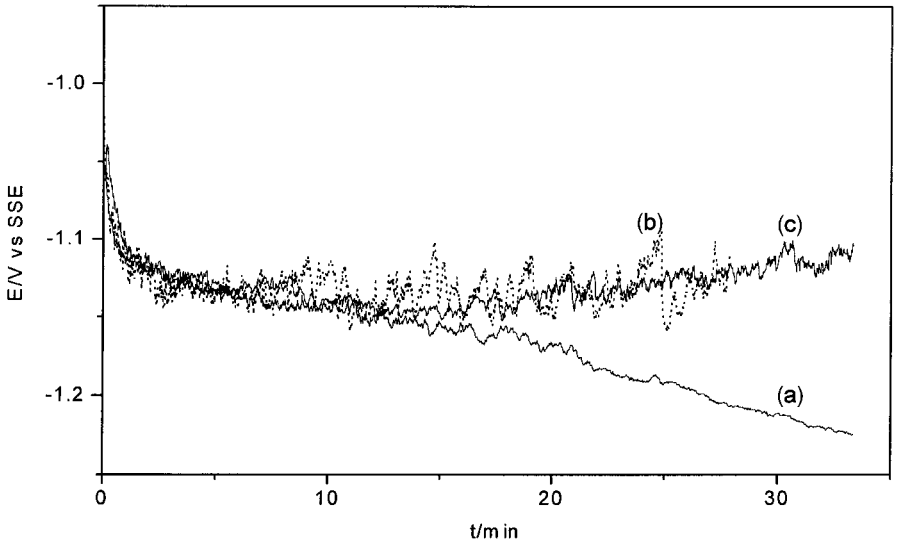

Fig. 14. Variation of the mixed potential of metallic zinc in CPE (Zn(CPE)) with the immersion time in aqueous solution containing 10^{-3} M NaCN and 0.01 M Na_2SO_4, at different concentrations of $(Au(CN)_2^-)$ and pH: (a) 10^{-6} M at pH 10, (b) 10^{-6} M at pH 11 and (c) 10^{-3} M at pH 10. E/t curves for the $Au(CN)_2^-/Zn^0$ system at two gold concentrations (10^{-6} M and 10^{-3} M $Au(CN)_2^-$) at pH 10 and 10^{-4} M CN^-.

conditions at pH 10 and when the ratio of cyanide to gold is large.

4. Conclusions

The following may be concluded with respect to zinc powder oxidation in cyanide solutions: initially the zinc powder is covered by a passive hydroxide coating which requires a large overpotential to dissolve. The characteristics of this layer are different at two distinct values of pH, being much more stable at pH 10 than at pH 11. At the latter pH, an oxidation–passivation process was observed using chronoamperometric and mixed potential measurement techniques. The formation and dissolution of the hydroxide layer is strongly affected by the pH.

Generally, it has been found that at high cyanide concentrations, gold reduction is limited by a diffusional process. However, at low cyanide concentrations, as those used in industrial practice, the present study determined that gold reduction is influenced by the competitive adsorption between the cyanide, hydroxyl and gold dicyanide ions. At high concentrations of gold in solution, cyanide is replaced by $Au(CN)_2^-$ on the electrode surface. However, in more alkaline solutions, gold adsorption is suppressed by the competition of hydroxyl ions for the same sites. At pH 10 and low cyanide concentration, the faradaic reduction of gold is evident only when this is present at the highest concentration (10^{-3} M).

Because gold reduction is completely concealed by the strong adsorptive processes, the construction of Evans'

diagrams from chronoamperometric curves does not reflect the cementation process and consequently, the mixed potentials obtained may not be valid. This was confirmed by the direct measurement of the mixed potentials. From these potentials it was possible to conclude that the controlling step of the cementation changes when the pH is modified from 10 to 11, where zinc oxidation determines the kinetics of the process. At pH 10, the kinetics are affected by the competitive adsorption between the gold dicyanide complex and the free cyanide ion. For this reason, a practical suggestion to obtain an optimum cementation velocity is to operate at a low pH value (pH 10) with a high cyanide to gold ratio.

Acknowledgements

The authors wish to thank CONACyT (Mexican National Science and Technology Foundation) for the postgraduate scholarship awarded to Soledad Vilchis-Carbajal.

References

1. J. Dorr and F. Bosqui, 'Cyanidation of Gold and Silver Ores' (McGraw-Hill, New York 1950), p. 184.
2. E.M. Hamilton, 'Manual of Cyanidation' (McGraw-Hill, New York, 1950).
3. M.C. Jha, *in* Proceedings of the First International Symposium on 'Precious Metals Recovery' Reno, Nevada, 10–14 June 1984, p. XXI-1.
4. B. Ihsan, B. Hermann and Y. Atila, *Erzmetall* **33** (1980) 399.
5. J.D. Miller, R.Y. Wan and J.R. Parga, 'Precious and Rare Metal Technologies', edited by A.E. Torma and I.H. Gundiler (Elsevier, Amsterdam, 1989), p. 281.
6. R.L. Paul and D. Howarth, Proceedings of the International Conference of Gold. Extractive Metallurgy of Gold (SAIMM, Johannesburg, 1986), p. 156.
7. M. Nicol, E. Schalch, P. Balestra and H. Hegedus, *J. South Afr. Inst. Min. Met.* **79** (1979) 191.
8. F. Lawson, *in* 'Thermodynamics and Kinetics of Metallurgical Processes' edited by M.M. Rao, K.P. Abraham, G.N.K. Iyengar, and R.M. Mallya (The Indian Institute of Metals, Calcutta, 1985), p. 207.
9. N.A. Sareyed-Dim and F. Lawson, *Trans. Inst. Min. Met.* **85** (1976) C1.
10. E.T. Eisenmann, *J. Electrochem. Soc.* **125** (1978) 717.
11. I. Lázaro, N. Martínez, I. Rodríguez, E. Arce and I. González, *Hydrometallurgy* **38** (1995) 277.
12. A.J. Bard, R. Parsons and J. Jordan, 'Standard Potentials in Aqueous Solution' (Marcel Dekker, New York, 1985), p. 254.
13. A.E. Martell and R.M. Smith, 'Critical Stability Constants' Vols 4 and 6 (Plenum Press, New York, 1976 and 1982).
14. W. Chrzanowski, Y. Li and A. Lasia, *J. Appl. Electrochem.* **26** (1996) 385.
15. D.M. MacArthur, *J. Electrochem. Soc.* **119** (1972) 672.
16. M. Miranda-Hernández and I. González, *Electrochim. Acta* **2** (1997) 2295.